Inactivation of epoxide hydrolase by catalysis-induced formation of isoaspartate

Bert van Loo, Hjalmar P. Permentier, Jaap Kingma, Helen Baldascini, Dick B. Janssen[*]

Biochemical Laboratory, Groningen Biomolecular Sciences and Biotechnology Institute, University of Groningen, Nijenborgh 4, 9747 AG Groningen, The Netherlands

Abstract **Epoxide hydrolases catalyze hydrolytic epoxide ring-opening, most often via formation of a covalent hydroxyalkyl-enzyme intermediate. A mutant of *Agrobacterium radiobacter* epoxide hydrolase, in which the phenylalanine residue that flanks the invariant catalytic aspartate nucleophile is replaced by a threonine, exhibited inactivation during conversion when the (*R*)-enantiomer of *para*-nitrostyrene epoxide was used as substrate. HPLC analysis of tryptic fragments of the epoxide hydrolase, followed by MALDI-TOF and TOF/TOF analysis, indicated that inactivation was due to conversion of the nucleophilic aspartate into isoaspartate, which represents a novel mechanism of catalysis-induced autoinactivation. Inactivation occurred at a lower rate with the (*S*)-enantiomer of *para*-nitrostyrene epoxide, indicating that it is related to the structure of the covalent hydroxyalkyl-enzyme intermediate.**
© 2008 Federation of European Biochemical Societies. Published by Elsevier B.V. All rights reserved.

Keywords: Epoxide hydrolase; Isoaspartate; Covalent modification; Enzyme inactivation

1. Introduction

Epoxide hydrolases catalyze conversion of epoxides to diols via a covalent hydroxyalkyl-enzyme intermediate [1–3]. This reaction is of great importance in the mammalian metabolism and detoxification of xenobiotic compounds [4]. Epoxide hydrolases can also be applied in industrial biocatalysis [5]. Most known epoxide hydrolases belong to the α/β-hydrolase fold family, which implies that they have a catalytic triad composed of a nucleophile, a histidine base, and an acidic amino acid. In epoxide hydrolases, haloalkane dehalogenases, and fluoroacetate dehalogenases the nucleophile is an aspartate, instead of the more common serine that is present in lipases and other esterases of this protein family [6].

During our studies with some mutant epoxide hydrolases that were found in a site-saturation library of *Agrobacterium radiobacter* epoxide hydrolase (EchA) at position 108, we observed that substrate conversion progress curves leveled off before complete conversion was achieved, and that the curves could not be described by Michaelis–Menten kinetics with product inhibition. This phenomenon indicated inactivation of the enzyme during catalysis (van Loo et al., unpublished re-

sults). Previous results showed that EchA was irreversibly inactivated during prolonged incubation with some diols that can be produced from epoxides, most notably 1,2-octanediol [7]. This inactivation could be prevented by addition of a competitive inhibitor, suggesting that inactivation was caused by interaction of the 1,2-diol in the active site. Although inactivation was mostly irreversible, mass spectrometry measurements indicated no net change in molecular mass during the inactivation process. Furthermore, circular dichroism (CD) measurements showed that no unfolding of the enzyme occurred, and only in the near-UV regions significant changes were observed, which were correlated to changes in the active site by comparison of spectra of wild-type and mutant enzymes [7].

In this paper, we address the mechanism of inactivation of an F108T mutant of EchA that is particularly sensitive to inactivation upon incubation with its substrate (*R*)-*para*-nitrostyrene oxide. Residue F108 distally flanks the nucleophilic aspartate and is conserved as a bulky group in α/β-hydrolase fold epoxide hydrolases. Kinetic measurements showed that inactivation occurred on average once in every 119 catalytic cycles and biochemical analysis of the inactivated enzyme suggests that the active-site nucleophilic aspartate is converted into isoaspartate.

2. Materials and methods

2.1. Materials

We used mutant EchA F108T that was obtained from a site-saturation library at position 108 (van Loo et al., manuscript in preparation). Production and purification of this mutant enzyme were done essentially as described by Rink et al. [3]. (*R*)-*para*-nitrostyrene epoxide ((*R*)-pNSO) and (*S*)-pNSO were a gift of Enzis. The purity was checked by HPLC (>98%). 1-(*R*)-*para*-nitrophenyl-1,2-ethanediol was prepared by hydrolysis of a solution of (*R*)-pNSO with epoxide hydrolase, followed by heat inactivation (10 min, 80 °C) and removal of protein by filtration. The preparation contained 90% (*R*)-diol and 10% (*S*)-diol as judged by chiral HPLC [8]. *Para*-nitrophenyl glycidylether was obtained from Acros.

2.2. Enzymatic conversions

Conversion of epoxides and activity assays were carried out with purified wild-type or F108T mutant epoxide hydrolase at 30 °C in 50 mM Tris · SO$_4$ buffer, pH 7.5, and followed at 310 nm (pNSO) or 350 nm (*para*-nitrophenyl glycidylether, pNPGE), as described previously [9]. In order to keep the absorbance of substrate at the start of the conversion below 1, the substrate concentration was lower than 250 μM in all experiments. Amounts of diol formed and activities were calculated from the decrease in absorbance (for pNSO, $\varepsilon_{310epoxide} = 4289 \ M^{-1} \ cm^{-1}$, $\varepsilon_{310diol} = 3304 \ M^{-1} \ cm^{-1}$ and for pNPGE, $\varepsilon_{350epoxide} = 4218 \ M^{-1} \ cm^{-1}$, $\varepsilon_{350diol} = 4889 \ M^{-1} \ cm^{-1}$). Enzyme reactivation was followed in the same Tris buffer.

[*]Corresponding author. Fax: +31 50 3634165.
E-mail address: D.B.Janssen@rug.nl (D.B. Janssen).

2.3. Circular dichroism measurements

Circular dichroism (CD) spectra of EchA F108T before and after incubation with (*R*)-pNSO were measured on an AVIV circular dichroism spectrometer (62ADS). Far-UV spectra were recorded at 25 °C from 190 to 250 nm in a 0.1 cm quartz cuvette using a bandwidth of 1 nm. Spectra obtained from three scans were averaged and were corrected for absorbance caused by the incubation solution. Near-UV CD spectra of wild-type and mutant epoxide hydrolases were recorded from 250 to 310 nm using a 0.5 cm quartz cuvette. The spectra of three scans, each recorded using a band width of 1 nm and steps of 1 nm, were averaged.

2.4. Tryptic cleavage of EchA F108T and HPLC analysis of digests

Purified EchA F108T, before and after incubation with (*R*)-pNSO, was dialyzed against 100 mM NaHCO$_3$, pH 8, and subsequently digested with 1% (w/w) of trypsin for 18 h at 37 °C. The digest was subjected to HPLC, which was carried out on a Nucleosil C18 column (5 μm, 250 × 2.1 mm) that was operated with a linear gradient of acetonitrile (0–70% (v/v), 1 ml min^{-1}, 60 min) in 0.1% (v/v) trifluoroacetic acid. Elution was followed at 214 nm and the target peptides were manually collected, lyophilized and used for mass spectrometric analysis.

2.5. Mass spectrometry of EchA F108T peptides

The isolated peptides were dissolved in 50% acetonitrile containing 0.1% (v/v) trifluoroacetic acid and mixed with an equal volume of 10 mg ml^{-1} α-cyano-4-hydroxycinnamic acid in the same solvent. Samples of 1.5 μl were spotted on the target and the samples were dried in air. MALDI-TOF and TOF/TOF mass spectra were recorded using a 4700 Proteomics Analyzer (Applied Biosystems, Foster City, CA, USA). Spectra were calibrated externally. Peptide fragmentation spectra were produced with a collision energy of 1 keV and air as collision gas at 1×10^{-6} Torr.

3. Results

3.1. Inactivation behavior of EchA F108T

Kinetic resolution experiments with purified F108T mutant epoxide hydrolase indicated that the enzyme became inactivated during conversion of *para*-nitrostyrene oxide (pNSO), although the protein was stable upon storage under the same conditions in the absence of substrate. The F108T enzyme exhibited enantioselectivity, but the conversion slowed down over time and stopped after 91% of the preferred (*R*)-enantiomer and 49% of the (*S*)-enantiomer of pNSO were hydrolyzed
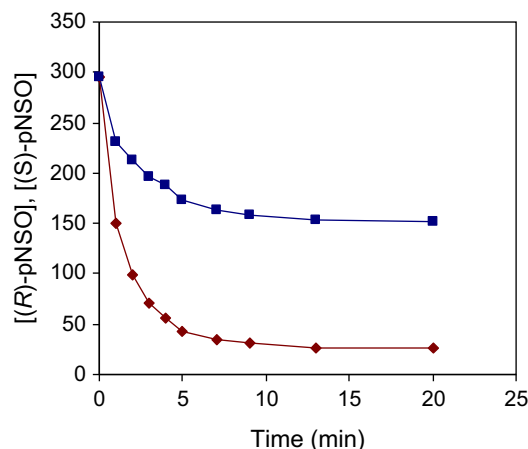

Fig. 1. Kinetic resolution of *rac*-pNSO and concomitant enzyme inactivation during turnover with F108T epoxide hydrolase (2.1 μM). Symbols: ◆, (*R*)-pNSO; ■, (*S*)-pNSO concentration.

(Fig. 1). When conversion stopped, the enzyme had performed only 197 turnovers.

To monitor the inactivation in more detail, varying amounts of F108T epoxide hydrolase were incubated with (*R*)-pNSO (170 μM), and hydrolysis of epoxide to diol was followed at 310 nm in a spectrophotometer. The amount of epoxide that was converted was proportional to the amount of enzyme added, indicating that only a limited number of substrate molecules was turned over per enzyme molecule. When more than 1.5 μM enzyme was added, all of the (*R*)-pNSO (>95%) was converted to its corresponding diol in 10 min (Fig. 2A). At enzyme concentrations below 1.5 μM, the amount of substrate converted was incomplete and proportional to the amount of enzyme added. The slope of the fitted curve, which is 119, is equal to the average number of conversions an enzyme molecule performs before it is inactivated, which can be called the transformation capacity.

The inactivation occurred faster with the preferred (*R*)-enantiomer of pNSO than with (*S*)-pNSO, and the calculated transformation capacity of F108T epoxide hydrolase with (*S*)-
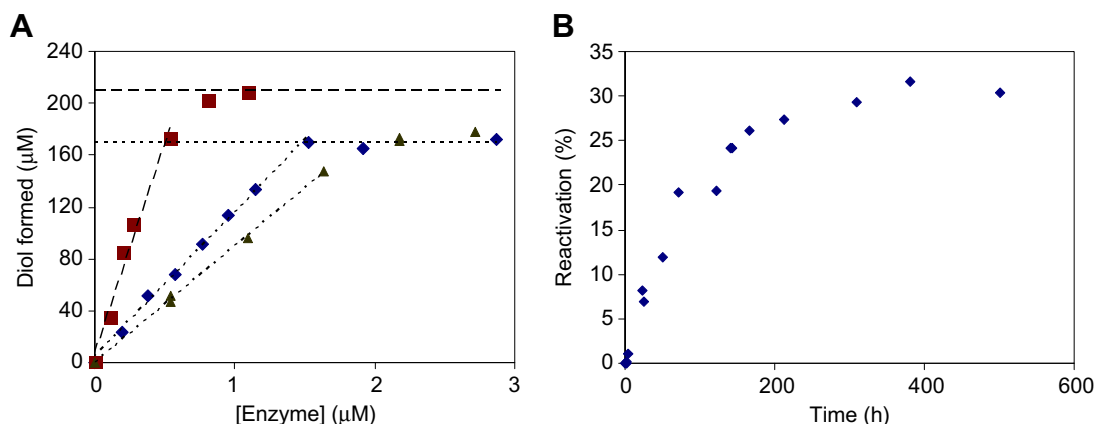

Fig. 2. Inactivation of F108T EchA by pNSO during substrate turnover. (A) Concentration of converted epoxide vs. the concentration of added enzyme for: (■), F108T EchA with 215 μM (*S*)-pNSO; (◆), F108T EchA with 170 μM (*R*)-pNSO; (▲), F108T EchA with 170 μM (*R*)-pNSO and 200 μM (*R*)-1-*p*-nitrophenyl-1,2-ethanediol. The slopes of the fitted curves (◆, 119; ■, 404) represent the average maximal turnovers per enzyme molecule (transformation capacity). Horizontal dashed and dotted lines indicate the level of diol formed in case of complete turnover of (*S*)-pNSO and (*R*)-pNSO, respectively. (B) Recovery of activity during storage of F108T EchA (5 μM) at 4 °C after removal of excess (*R*)-pNSO by dialysis.

pNSO was 404. When the F108T mutant epoxide hydrolase was incubated with (R)-pNSO in the presence of excess of the product 1-((R)-p-nitrophenyl)-1,2-ethanediol (170 μM), inactivation proceeded only somewhat faster than with (R)-pNSO alone. Incubation of F108T EchA (5.4 μM) with 170 μM diol during 20 min at 30 °C also did not lead to a decrease in enzyme activity (specific activity 10 ± 0.2 U/mg protein with pNPGE). Thus, the observed inactivation is not due to a normal product inhibition. Instead, it must be caused by substrate turnover. When wild-type enzyme (0.035 μM) was incubated with 314 μM (R)-pNSO, >95% conversion occurred in 20 min, in agreement with a k_{cat} of 2.4 s^{-1} and a transformation capacity exceeding 10 000, showing that wild-type EchA was not sensitive to this substrate-turnover induced inactivation.

The inactivation process observed with the F108T mutant was partially reversible. When protein that was inactivated with (R)-pNSO was dialyzed to remove remaining substrate and stored at 4 °C, up to 30% of the activity was regained in 12 days, after which no further activity increase was observed (Fig. 2B).

Biochemical characterization of the F108T mutant EchA before and after inactivation by (R)-pNSO by far-UV circular dichroism (CD) (Fig. 3A) indicated that unfolding events were not the cause of the inactivation since α-helix and β-sheet content did not change. Near-UV CD spectra, however, indicated

that the direct environment of aromatic residues in and near the active site had changed significantly (Fig. 3B). Initial analysis of peptide samples obtained by tryptic cleavage showed no gross changes in the digestion pattern, and no indication for cross linking was obtained. These observations indicated that a subtle covalent modification, which did not result in a large change of the molecular weight or a major unfolding event, was responsible for the observed conversion-induced inactivation process.

3.2. Mass spectrometric analysis

To further analyze the biochemical cause of the inactivation, samples of native F108T EchA and of protein that was incubated with (R)-pNSO were digested with trypsin and analyzed by reverse phase HPLC (Fig. 4). The only clear difference that could be observed was the elution of an additional small peak for the peptide digest of the inactivated enzyme (b1, elution time 30.7 min). The differences in the peaks around 45 min were caused by slight retention time variations or incomplete digestion, and no peptides of interest were observed in them. The 30.7 min peak which preceded a large peak that was present in both spectra (a2 and b2), was absent in the native enzyme (Fig. 4). Mass spectrometric analysis by MALDI-TOF of this peptide (b1) indicated that it had a protonated mass of 1593.9 Da. The same mass was found in the larger peaks b2 and a2, which eluted just after peak b1, as well as for the
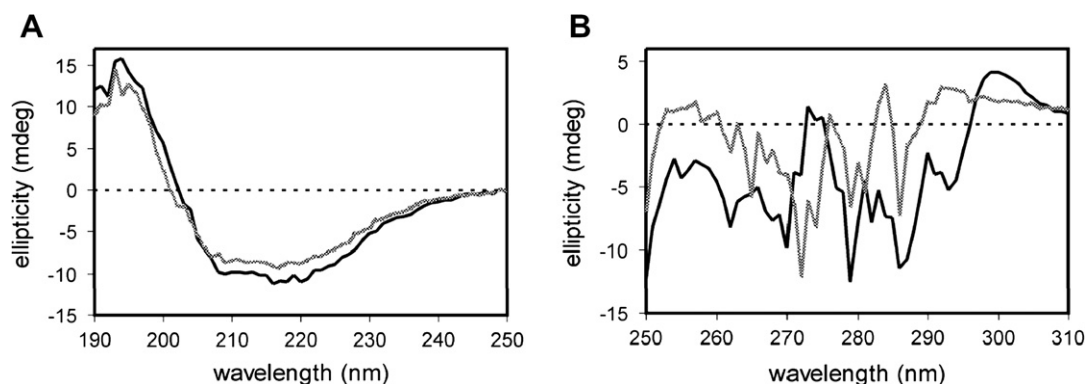

Fig. 3. Circular dichroism (CD) spectra for EchA F108T before (black line) and after (gray line) incubation with (R)-pNSO. (A) Far UV CD spectra in showing that no major structural changes were the cause of the inactivation. (B) Near-UV spectra pointing to a small local change in environment.
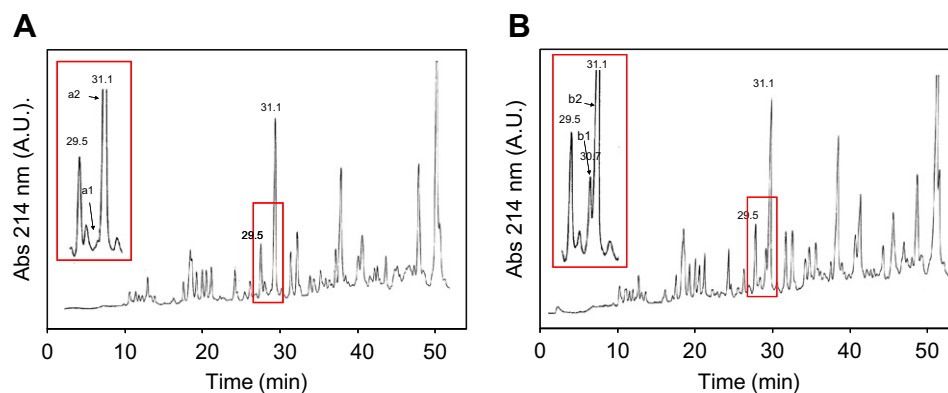

Fig. 4. HPLC elution pattern of tryptic digests of native EchA F108T (A) and of EchA F108T exposed to (R)-pNSO (B). The peak that appears with inactivated enzyme at 30.69 min (b1) is missing in the native enzyme (a1). This peptide and the next eluting peptide, represented by the largest peaks in the insets (a2, b2), were analyzed by MALDI-TOF MS.

material collected as a small shoulder (a1) at the same retention time as b1, which presumably contains 1593.9 material from the a2 peak. The major component of peaks b2 and a2 was a different peptide with a protonated mass of 1227.6 Da. The 1593.9 Da peak corresponds to the tryptic peptide AYVVGHDTAAIVLHK, which harbors the active-site nucleophile, aspartate 107. Thus, the retention time of this peptide as it is present in peak b1 has changed as compared to the original peptide (at positions a2 and b2), but without a change in net mass.

One possible covalent modification that we considered is rearrangement of Asp107 to form isoaspartate. Isoaspartate linkages are known to be formed in some proteins via succinimide-linked deamidation of asparagines and rearrangement of aspartic acids [10]. Such a modification can be detected by tandem mass spectrometry [11–13]. The MALDI-TOF/TOF fragmentation spectra of the peptide corresponding to peak b1 indeed showed a pattern that clearly differed from that of the other three peptides (Fig. 5A).

The spectrum from the inactivated peptide (b1) showed a clear decrease in intensity of the b_8, b_9 and b_{10}-ions and an increase in intensity of the y_8 and y_9-ions (Fig. 5B), as compared to the control peptides (a1, a2, b2). The respective b- and y-ion masses of all four peptides are the same, but the distinct difference in intensities strongly suggests that peptide b1, from the modified and inactivated protein, is structurally different from the control peptides. Most significantly, the peptide yielded an additional, unique fragment that is generated by loss of HCOOH from the y_9 ion ($\Delta m = 46$ Da, peak d in Fig. 5B), which has isoaspartate as the N-terminal residue. During molecular fragmentation, loss of the α-carboxylic acid moiety of isoaspartic acid is more favorable than loss of the β-carboxylic acid group from aspartic acid [12,13]. Gogichaeva et al. [14] have found that this is a general difference in fragmentation of α- and β-amino acids by MALDI-TOF/TOF. The observation of the isoaspartate-specific fragment clearly shows

the generation of isoaspartate and indicates that this is the mechanism of the observed enzyme inactivation.

The putative succinimide intermediate, with a protonated mass of 1575.9 Da, was not observed by MALDI-TOF. Since the analysis was performed under acidic conditions, the succinimide is expected to be hydrolyzed to aspartate/isoaspartate. The control peptides do not show any isoaspartate (as judged from the absence of the y_9-46 fragment peak). It is possible that (some of) the inactivated protein contained the succinimide intermediate which would subsequently be hydrolyzed during sample preparation. Since both aspartate and isoaspartate can be formed by hydrolysis, this would underestimate the amount of modified peptide and protein.

4. Discussion

A peculiar observation with EchA F108T was that it quickly underwent inactivation during turnover of *para*-nitrostyrene epoxide. This phenomenon was only observed when the (R)-enantiomer was converted and could be described as a partitioning process in which enzyme either became inactivated or converted substrate catalytically. The average number of catalytic cycles leading to inactivation was 119. The inactivation was also not observed with wild-type enzyme and was influenced by the stereoconfiguration of the substrate. The (S)-enantiomer was converted more slowly and a much lower rate of inactivation was found.

HPLC and mass spectrometry only suggested a single change in the peptide profile of the inactivated protein: the nucleophilic aspartate in the native enzyme was converted into an isoaspartate in the (R)-pNSO-exposed enzyme. This was clearly indicated by the loss of a carboxylic acid group in the peptide that originated from inactivated EchA F108T, as well as by the reduction in intensity of b fragments and the increase in intensity of y fragments in the MS/MS fragmentation spec-
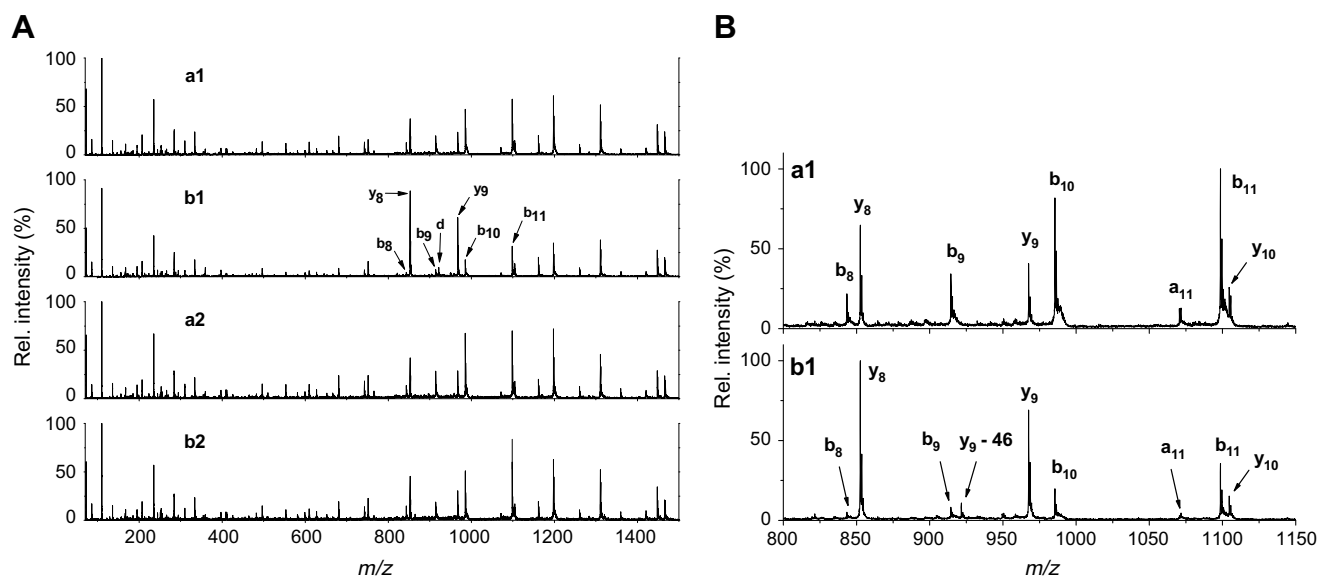

Fig. 5. MALDI-TOF/TOF fragmentation spectra of the 1593.9 Da peptides isolated by HPLC. The peptide sequence is AYVVGHDTAAIVLHK. (A) Peptides from active enzyme (HPLC peaks a1 and a2) and enzyme inactivated with (R)-pNSO (HPLC peaks b1 and b2). (B) The fragments detected from peak b1 show a decreased intensity of the b-ions, and an increased intensity of the y-ions, indicated with arrows. Furthermore, an isoaspartate specific fragment (d) formed by decarboxylation (y_9-46 Da) is observed only in peak b1.

trum. These changes are typically observed in peptides that contain isoaspartic acid [11–13].

We propose that the inactivation is caused by a rearrangement of the covalent alkyl-enzyme intermediate that is formed during the first half reaction of the catalytic cycle, which is epoxide ring-opening. Dependent on the nature of the substrate, the hydroxyalkyl-intermediate of the F108T mutant enzyme would occasionally be cleaved by intramolecular nucleophilic attack by the backbone amide nitrogen of the amino acid distal to the active-site aspartate. This reaction is similar to the one that spontaneously occurs in some proteins in which isoaspartate linkages are formed between Asp/Asn and their distal residues via a succinimide intermediate [10]. Hydrolysis of the intermediate would lead either to reactivated enzyme, or to formation of isoaspartic acid (Fig. 6). The fact that this phenomenon is observed in a mutant enzyme and hardly in the wild-type enzyme, which respectively have a threonine and phenylalanine flanking the nucleophilic aspartate, is in agreement with the effect that side chains of residues distally flanking Asn or Asp residues can have on the acidity of the backbone amide that is involved in the formation of the succinimide intermediate [15]. The nitrogen that performs the nucleophilic attack that results in the formation of the intermediate is more easily deprotonated and therefore more nucleophilic at alkaline to neutral pH if a residue such as serine or threonine is present instead of a more apolar residue such as phenyl alanine [15]. The nature of the reactivation process, which is only partial and proceeds slowly, may be cleavage of the succinimide intermediate to active enzyme, although this has not been proven.

Formation of succinimide intermediates and isoaspartic groups in proteins have been observed in many cases [16–18] most notably during aging of a protein, but has, to our knowledge, not been associated with a catalytic event in an enzyme active-site. The results descr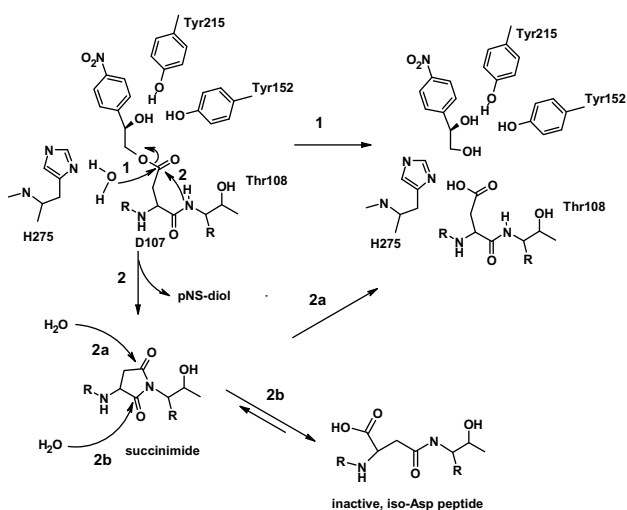ibed here thus identify a novel mechanism by which an enzyme that possesses a nucleophilic aspartate may become inactivated. If this mechanism also is of importance for other enzymes that rely on formation of covalent intermediates involving an aspartate remains to be established. We have observed that the slow inactivation that is observed when wild-type EchA is exposed to some 1,2-diols (products) is accompanied by alterations in the CD spectrum and irreversible loss of activity without unfolding or changes in molecular mass [7], which suggests that high concentration of product may evoke similar inactivating modifications in the active site of an epoxide hydrolase, possibly by formation of a covalent or non-covalent enzyme-product complex.

Fig. 6. Mechanism of inactivation of F108T epoxide hydrolase upon incubation with (R)-pNSO. We propose that (R)-pNSO can act as a substrate when the covalent intermediate is cleaved in the normal way (route 1). However, instead of water, the backbone amide nitrogen of the residue distal to the aspartate may perform a nucleophilic attack on the carbonyl carbon of the alkyl-enzyme intermediate. This produces a succinimide intermediate, that may undergo hydrolysis to reform native enzyme (route 2a, reactivation) or it may be cleaved at the main chain carbonyl function, which produces an isoaspartate residue in the main chain at position D107 (route 2b).

References

[1] Tzeng, H.-F., Laughlin, L.T., Lin, S. and Armstrong, R.M. (1996) The catalytic mechanism of microsomal epoxide hydrolase involves reversible formation and rate-limiting hydrolysis of the alkyl-enzyme intermediate. J. Am. Chem. Soc. 118, 9436–9437.

[2] Arand, M., Grant, D.F., Beetham, J.K., Friedberg, T., Oesch, F. and Hammock, B.D. (1994) Sequence similarity of mammalian epoxide hydrolases to the bacterial haloalkane dehalogenase and other related proteins. Implication for the potential catalytic mechanism of enzymatic epoxide hydrolysis. FEBS Lett. 338, 251–256.

[3] Rink, R., Fennema, M., Smids, M., Dehmel, U. and Janssen, D.B. (1997) Primary structure and catalytic mechanism of the epoxide hydrolase from *Agrobacterium radiobacter* AD1. J. Biol. Chem. 272, 14650–14657.

[4] Morisseau, C. and Hammock, B.D. (2005) Epoxide hydrolases: mechanisms, inhibitor designs, and biological roles. Annu. Rev. Pharmacol. Toxicol. 45, 311–333.

[5] Orru, R.V., Archelas, A., Furstoss, R. and Faber, K. (1999) Epoxide hydrolases and their synthetic applications. Adv. Biochem. Eng. Biotechnol. 63, 145–167.

[6] Ollis, D.L., Cheah, E., Cygler, M., Dijkstra, B., Frolow, F., Franken, S.M., Harel, M., Remington, J., Silman, I., Schrag, J., Sussman, J.L., Verschueren, K. and Goldman, A. (1992) The α/β-hydrolase fold. Protein Eng. 5, 197–211.

[7] Baldascini, H. (2005) Bioreaction engineering for the kinetic resolution of racemic epoxides by epoxide hydrolases. Ph.D. Thesis, University of Groningen.

[8] Lutje Spelberg, J.H., Rink, R., Kellogg, R.M. and Janssen, D.B. (1998) Enantioselectivity of a recombinant epoxide hydrolase from *Agrobacterium radiobacter*. Tetrahedron Asymmetry 9, 3081–3084.

[9] Rink, R., Lutje Spelberg, J.H., Pieters, R.J., Kingma, J., Nardini, M., Kellogg, R.M., Dijkstra, B.W. and Janssen, D.B. (1999) Mutation of tyrosine residues involved in the alkylation half reaction of epoxide hydrolase from *Agrobacterium radiobacter* AD1 results in improved enantioselectivity. J. Am. Chem. Soc. 121, 7417–7418.

[10] Reissner, K.J. and Aswad, D.W. (2003) Deamidation and isoaspartate formation in proteins: unwanted alterations or surreptitious signals? Cell. Mol. Life Sci. 60, 1281–1295.

[11] De Boni, S., Oberthür, C., Hamburger, M. and Scriba, G.K.E. (2004) Analysis of aspartyl peptide degradation products by high-performance liquid chromatography and high-performance liquid chromatography–mass spectrometry. J. Chromatogr. A 1022, 95–102.

[12] Krokhin, O.V., Antonovici, M., Ens, W., Wilkins, J.A. and Standing, K.G. (2006) Deamidation of -Asn-Gly- sequences during sample preparation for proteomics: consequences for MALDI and HPLC–MALDI analysis. Anal. Chem. 78, 6645–6650.

[13] Gonzalez, L.J., Shimizu, T., Satomi, Y., Betancourt, L., Besada, V., Padron, G., Orlando, R., Shirasawa, T., Shimonishi, Y. and Takao, T. (2000) Differentiating α- and β-aspartic acids by

electrospray ionization and low-energy tandem mass spectrometry. Rapid Commun. Mass Spectrom. 14, 279–284.

[14] Gogichaeva, N.V., Williams, T. and Alterman, M.A. (2007) MALDI-TOF/TOF tandem mass spectrometry as a new tool for amino acid analysis. J. Am. Soc. Mass Spectrom. 18, 279–284.

[15] Radkiewicz, J.L., Zipse, H., Clarke, S. and Houk, K.N. (2001) Neighboring side chain effects on asparaginyl and aspartyl degradation: an ab initio study of the relationship between peptide conformation and backbone NH acidity. J. Am. Chem. Soc. 123, 3499–3506.

[16] Fujii, N., Momose, Y., Ishibashi, Y., Uemura, T., Takita, M. and Takehana, M. (1997) Specific racemization and isomerization of the aspartyl residue of αA-crystallin due to UV-B irradiation. Exp. Eye Res. 65, 99–104.

[17] Najbauer, J., Orpiszewski, J. and Aswad, D.W. (1996) Molecular aging of tubulin: accumulation of isoaspartyl sites *in vitro* and *in vivo*. Biochemistry 35, 5183–5190.

[18] Paranandi, M.V., Guzzetta, A.W., Hancock, W.S. and Aswad, D.W. (1994) Deamidation and isoaspartate formation during in vitro aging of recombinant tissue plasminogen activator. J. Biol. Chem. 269, 243–253.